ϵ_p: particle porosity
λ: specific heat of evaporation, kcal·kg^{-1}
ρ_s: molar density of solid
σ: standard deviation
τ: dimensionless time, $t/t_{0.5}$
θ: dimensionless temperature, T/T_0
ψ: structural parameter, defined by Bhatia and Perlmutter (1983)

Registry No. $Ca(OH)_2$, 1305-62-0.

Literature Cited

Beruto, D.; Barco, L.; Searcy, A. W.; Spinolo, G. Characterization of the porous CaO particles formed by decomposition of $CaCO_3$ and $Ca(OH)_2$ in vacuum. *J. Am. Ceram. Soc.* **1980**, *63*, 439-443.

Bhatia, S. K.; Perlmutter, D. D. A random-pore model for fluid-solid reaction II: Diffusion and transport effect. *AIChE J.* **1981a**, *27*, 247-254.

Bhatia, S. K.; Perlmutter, D. D. The Effect of Pore Structure on Fluid-Solid Reactions: Application to the SO_2 lime Reaction. *AIChE J.* **1981b**, *27*, 226-234.

Bhatia, S. K.; Perlmutter, D. D. Unified treatment of structural effects in fluid-solid reactions. *AIChE J.* **1983**, *29*, 281-289.

Borgwardt, R. H.; Bruce, K. R. Effect of Specific Surface Area on the Reactivity of CaO with SO_2. *AIChE J.* **1986**, *32*, 239-246.

Bruce, K. R.; Gullet, B. K.; Beach, L. O. Comparative SO_2 reactivity of CaO Derived from $CaCO_3$ and $Ca(OH)_2$. *AIChE J.* **1989**, *35*, 37-41.

Criado, J. M.; Morales, J. On the thermal decomposition mechanism for the dehydroxylation of alkaline earth hydroxides. *J. Thermal Anal.* **1976**, *10*, 103-110.

Doraiswamy, L. K.; Sharma, M. M. Gas-Solid Noncatalytic Reactions: Analysis and Modeling. Gas-Solid and Solid-Solid Reactions. *Heterogeneous Reactions: Analysis, examples, and reactor design*; John Wiley & Sons, Inc.: New York, 1984; Vol. 1.

Halstead, P. E.; Moore, A. E. The thermal dissociation of calcium hydroxide. *J. Chem. Soc.* **1957**, 3873-3875.

Jorgensen, C.; Chang, C. S.; Brna, T. G. Evaluation of sorbents and additives for dry SO_2 removal. *Environ. Prog.* **1987**, *6*, 26-32.

Klingspor, J.; Karlsson, H. T.; Bjerle, I. A kinetic study of the dry SO_2-limestone reaction at low temperature. *Chem. Eng. Commun.* **1983**, *22*, 81-103.

Lachapelle, D. G. EPA's LIMB technology development program. *Chem. Eng. Prog.* **1985**, *81*, 52.

Mai, M. C.; Edgar, T. F. Surface Area Evolution of Calcium Hydroxide During Calcination and Sintering. *AIChE J.* **1989**, *35*, 30-36.

Matsuda, H.; Ishizu, T.; Lee, S. K. Kinetic study of $Ca(OH)_2$/CaO reversible thermochemical reaction for thermal energy storage by means of chemical reaction. *Kagaku Kogaku Ronbunshu* **1985**, *11*, 542-548.

Marsh, A. W.; Ulrichson, D. L. Rate and diffusional study of the reaction of calcium oxide with sulfur dioxide. *Chem. Eng. Sci.* **1985**, *40*, 423-433.

Mu, J.; Perlmutter, D. D. Thermal decomposition of carbonates, carboxylates, oxalates, acetates, formates and hydroxides. *Thermochim. Acta* **1981**, *49*, 207-218.

Ortiz, M. I.; Viguri, J.; Irabien, A. Generación de energía y contaminación por SO_2. Tecnologías de control. *Energía* **1987**, *2*, 75-88.

Simons, G. A.; Garman, A. R.; Boni, A. A. The kinetics rate of H_2S sorption by CaO. *AIChE J.* **1987**, *33*, 211-217.

Szekely, J.; Evans, J. W.; Sohn, H. Y. Porous solids of unchanging overall sizes. *Gas-Solid Reactions*; Academic Press: New York, 1976.

Viguri, J. R. Hidróxido de calcio como reactivo en desulfuración de gases: Deshidratación y sinterización. Ph.D. Dissertation, The University of País Vasco, Bilbao, Spain, 1989.

Viguri, J.; Ortiz, I.; Irabien, A. Desulfuración de gases. Caracterización de calizas y derivados. *Abstracts of Papers*, 10th Encontro Anual da Sociedade Portuguesa de Química; Sociedade Portugesa de Quimica: Oporto 1987; pp 509-510.

Viguri, J. R.; Diego, L. F.; Ortiz, I.; Irabien, A. Desulfuración de gases. Conversión máxima de compuestos cálcicos. *Abstracts of Papers*, XXII Reunión Bienal de la Real Sociedad Española de Química; R.S.E.Q.: Murcia, 1988; p 382.

Received for review August 25, 1989
Revised manuscript received March 14, 1990
Accepted April 3, 1990

Thermal Dehydration of Calcium Hydroxide. 2. Surface Area Evolution

Angel Irabien,* Javier R. Viguri, Fernando Cortabitarte, and Inmaculada Ortiz
Departamento de Ingeniería Química, Facultad de Ciencias, Universidad del País Vasco, Apdo. 644, Bilbao 48080, Spain

The evolution of the specific surface area associated with the thermal decomposition of calcium hydroxide has been studied experimentally and described by kinetic models utilizing two different solids: commercial calcium hydroxide ($S_0 \approx 8.3$ m^2·g^{-1}) and calcium hydroxide reagent ($S_0 \approx 18.7$ m^2·g^{-1}). The surface area was observed to vary linearly with the fraction decomposed during the dehydration period. Sintering phenomena have been experimentally measured by treating calcium oxide samples ($S_0 \approx 46$ m^2·g^{-1}), obtained after dehydration of calcium hydroxide under constant conditions, at temperatures in the range 500–900 °C for periods of time up to 24 h. A previously developed model, German and Munir (1976), fits the experimental results well if the surface area decreases to less than 55% of the initial value. An empirical kinetic model, where the surface area is linearly related to the heating time, correlates the experimental data, when $\Delta S/S_0 \geq 55\%$. Simulated curves using the obtained kinetic models and parameters, for the specific surface during dehydration and sintering, agree well within the experimental results.

Introduction

Structural changes that take place during the thermal decomposition of calcium hydroxide to give calcium oxide are fundamentally related to the transport processes occurring in some of its reactions with gases that form a solid product. Due to its technological importance, sulfation is the most thoroughly studied reaction of this type.

When calcium hydroxide is thermally treated at intermediate temperatures (350–550 °C), the solid product shows a higher specific surface area than does the initial reagent. Surface generation depends on the kinetics of dehydration; at long times or when decomposition of the initial solid takes place at high temperatures, changes in the surface area and porosity due to sintering phenomena are of considerable importance, decreasing the specific

* Author to whom correspondence should be addressed.

0888-5885/90/2629-1606$02.50/0

surface area and consequently the reactivity with gases.

In a previous work (Irabien et al., 1990), conversion–time evolution in the thermal dehydration of calcium hydroxide was successfully described by means of a pseudohomogeneous model accounting for the kinetics of the surface reaction, external diffusion, and interparticle diffusion.

Borgwardt (1989) studied the sintering of nascent calcium oxide obtained from thermal decomposition of $CaCO_3$ and $Ca(OH)_2$ at temperatures above 700 °C; the model proposed by German and Munir (1976) correlated sintering kinetics, and lattice diffusion was identified as the mechanism of solid transport. Mai and Edgar (1989) analyzed the surface are evolution of calcium hydroxide during calcination and sintering at 1275 and 1425 K.

In this work, surface area changes associated with calcium hydroxide dehydration at medium temperatures (400–500 °C) have been experimentally measured using solids with different microstructures (commercial product, $S_0 = 8.3\ m^2 \cdot g^{-1}$ and reagent, $S_0 = 18.7\ m^2 \cdot g^{-1}$); the surface area was observed to vary linearly with the decomposed fraction, which can be described by a pseudohomogeneous kinetic model.

Calcium oxide, $S_0 = 46\ m^2 \cdot g^{-1}$, obtained by decomposition of commercial calcium hydroxide at 450 °C for 30 min, was used in the sintering study.

The initial rates of sintering corresponding to experiments performed between 500 and 900 °C allow the estimation of the quantitative surface area decrease when it is utilized as the sorbent reagent in flue gas desulfurization processes. From the fundamentals at a sufficiently high temperature, a system of solid particles undergoes a spontaneous process to become more compact, in which the surface area and the total volume decrease. The singering process may occur rather far below the melting point of the system (mp of CaO = 2500 °C). The initial stage of the sintering occurs when the connecting necks between the particles that touched at single points begin to grow. Further, pores are closed between the particles and have a tendency to shrink. Complete disappearance of pores is a lengthy process, and the final stages of sintering may be complicated by recrystallization.

Many efforts have been directed toward the kinetic description of sintering based on analytical expressions of the mass flux, which occurs between sites with positive and negative curvature. Discrepancies between the theory and the experimental results have led to the development of sintering models, in which diffusion of vacancies from places with a negative surface curvature toward the particle center is the controlling process (Sestak, 1984).

Under the consideration that the driving force for sintering is the excess surface energy over some value that would be finally attained at the temperature considered and as surface energy is proportional to surface area, Nicholson (1965) proposed the following sintering model:

$$dS/dt = -K_T(S - S_f) \tag{1}$$

where K_T is a constant depending on the temperature and S_f is the surface area finally attained. Some experimental results available on the change of surface area with time during the sintering of some oxides (MgO, Fe_2O_3) fit eq 1 well when a reasonable choice of S_f was made (Nicholson, 1965). Previous investigations have indicated second-order kinetics (Bortz et al., 1986; Silcox et al., 1986; Cole et al., 1986; Mai and Edgar, 1989) for calcium oxide sintering.

Empirical relations between S and t are also found in the literature (Gregg et al., 19855):

$$dS/dt = -K_S S t^{-n} \tag{2}$$

where $0 < n < 1.0$.

German and Munir (1976) formulated a standard two-sphere model of sintering particles to develop a kinetic relationship for surface area reduction. This model assumes that the grains have an initial spherical shape with multiple points of contact between adjacent grains. As sintering begins, a connecting neck forms at each point of contact and grows in diameter as matter is transported to the neck region under the influence of its curvature gradient. The transport necessary for neck growth occurs by one of four possible mechanisms. The specific surface area is reduced by an amount proportional to the neck diameter and the number of initial contact points between grains. The following generalized expression was derived for this process:

$$\left(\frac{S_0 - S}{S_0}\right)^{\gamma_S} = K_i t \tag{3}$$

where S_0 is the initial specific surface area, S is the specific surface area at time t, and K_i includes the diffusion coefficient (a function of temperature), surface tension, and other constants. The exponent γ_s has unique values for the different transport mechanisms, which are as follows: plastic flow, $\gamma_S = 1.1$; lattice diffusion, $\gamma_S = 2.7$; grain boundary diffusion, $\gamma_S = 3.3$; and surface diffusion, $\gamma_S = 3.5$.

The assumptions on which eq 3 is formulated are valid to a 50% reduction in surface area, at which neck overlap occurs and other surface reduction processes may become dominant. The exponent is also slightly dependent on the grain coordination number, which may change with particle density. This model has been successfully applied to describe isothermal sintering kinetics of Al_2O_3, ZnO, Fe_2O_3, TiO_2, and, recently, nascent calcium oxide (Borgwardt, 1989); in most cases, the transport mechanism deduced from the evaluation of γ_S is in agreement with the mechanism established by other experimental methods.

Experimental Section

Two different types of solids with different structural characteristics have been used to analyze the evolution of surface area when the solid is thermally treated: commercial calcium hydroxide, Dolomitas del Norte, S.A., $S_0 = 8.3\ m^2 \cdot g^{-1}$; and calcium hydroxide reagent obtained in the laboratory, $S_0 \approx 18.7\ m^2 \cdot g^{-1}$.

The experimental setup consists of a tubular reactor made of quartz located inside an electric oven and provided with downflow circulation of a preheated gas and heating rate control by a thermocouple situated in the middle of the reactor.

Extrapure nitrogen (>99.99%) after water saturation at $T = 288$ K, $p_w = 1.683 \times 10^{-2}$ atm, $T = 293$ K, $p_w = 2.307 \times 10^{-2}$ atm, and $T = 298$ K, $p_w = 3.126 \times 10^{-2}$ atm was preheated at the temperature of the experiment and was passed through the reactor at 50 $mL \cdot min^{-1}$.

The experimental system was checked with 1.25 g of inert silica for control purposes to establish the temperature (±1 K), showing a maximum heating rate of 50 $K \cdot min^{-1}$.

Experiments were performed with a 1.25-g sample (1 g of inert silica; 0.25 g of calcium hydroxide). No weight loss nor specific surface area change was observed for temperatures below 623 K, in the experimental range of partial pressure of water of 1.683×10^{-2} atm $\le p_w \le 3.126 \times 10^{-2}$ atm. Working with a maximum heating rate of 50 $K \cdot min^{-1}$, the heating period was subtracted from the reaction time, being $t = 0$ when the temperature reached 623 K.

After conclusion of the prescribed period, the reactor was cooled to 373 K and the sample was withdrawn, cooled

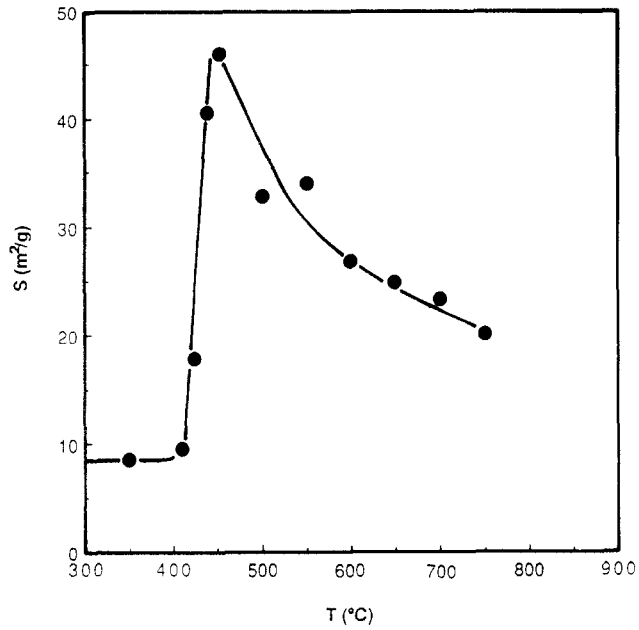

Figure 1. Surface area–temperature evolution for commercial $Ca(OH)_2$ dehydration during 30 min.

under inert atmosphere, weighted, and transferred (including inert silica, $S \leq 0.2$ $m^2 \cdot g^{-1}$) to a BET flask for surface area analysis carried out by nitrogen adsorption at 77 K using the standard BET method. Further details are given elsewhere (Viguri, 1989).

Kinetics and Modeling

Some preliminary experiments were carried out to analyze the evolution of surface area with temperature in the thermal decomposition of calcium hydroxide at $p_w = 2.307 \times 10^{-2}$ atm. A constant heating time of 30 min was used in the range between 673 and 1073 K; the results plotted in Figure 1 were obtained. Similar results were reported by Feugier (1986) for the variation of the specific surface area during calcination of $Ca(OH)_2$, $CaCO_3$, $MgCO_3$, and $CaCO_3$, simulating their behavior when they were utilized as solid sorbents for sulfur recovery during fluidized bed combustion.

The maximum observed in the curve of Figure 1 was attributed to the lumping between two different phenomena: (i) surface area generation during dehydration of calcium hydroxide to give a highly porous calcium oxide and (ii) surface area reduction due to sintering. The heating time also had an influence on the maximum value of the surface area attained; therefore, the heated samples reached a defined specific surface area depending on the thermal treatment.

From these results, it was concluded that it was necessary to analyze the increase of surface area due to the dehydration of $Ca(OH)_2$ and the decrease in surface area due to sintering phenomena:

$$A \xrightarrow[\text{dehydration}]{} B \xrightarrow[\text{sintering}]{} B_S \quad (4)$$
$$\uparrow W$$

Kinetic Modeling of the Surface Area Generation. The influence of the partial pressure of water was checked in the experiments performed with high surface calcium hydroxide at 698 K, $p_w = 3.126 \times 10^{-2}$ atm, and $p_w = 1.683 \times 10^{-2}$ atm, leading to the experimental values shown in Table I.

The influence of the temperature in the surface area generation was studied in experiments performed at 683 and 713 K under constant conditions of an intermediate

Table I. Influence of the Partial Pressure of Water in Experiments with High Surface Area Calcium Hydroxide at 698 K

	$p_w = 3.126 \times 10^{-2}$ atm		$p_w = 1.683 \times 10^{-2}$ atm	
time, min	loss of wt, %	S_g, $m^2 \cdot g^{-1}$	loss of wt, %	S_g, $m^2 \cdot g^{-1}$
5	0.59	19.4	0.75	18.3
10	3.61	19.8	5.05	21.8
15	7.12	22.5	8.23	26.8
20	14.1	30.4	15.3	34.4

Table II. Experiments Performed at Different Temperatures and Constant Partial Pressure of Water ($p_w = 2.307 \times 10^{-2}$ atm)

	T = 683 K		T = 713 K	
time, min	loss of wt, %	S_g, $m^2 \cdot g^{-1}$	loss of wt, %	S_g, $m^2 \cdot g^{-1}$
5	0.096	17.8	1.05	19.3
10	2.36	19.5	4.22	21.1
15	5.87	23.9	10.14	26.9
20	11.96	30.0	13.4	29.1
25			15.62	33.8

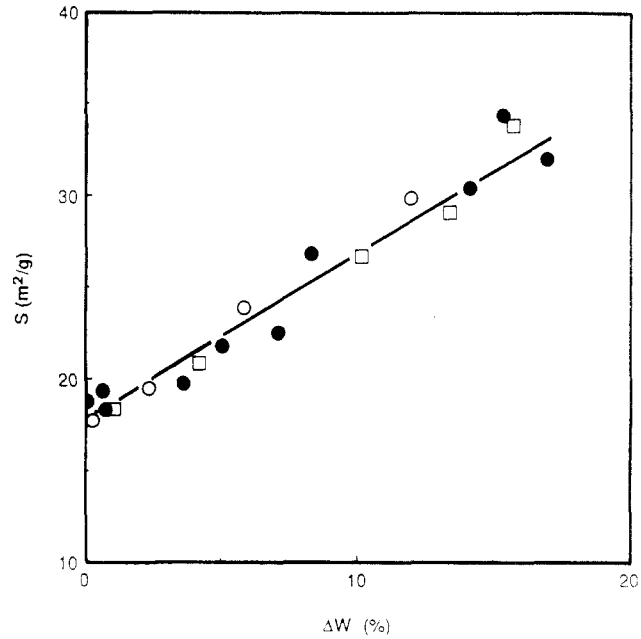

Figure 2. Surface area–weight loss evolution for $Ca(OH)_2$ reagent. 1.683×10^{-2} attm $\leq p_w \leq 3.126 \times 10^{-2}$ atm; (○) T = 410 °C; (●) T = 425 °C; (□) T = 440 °C.

partial pressure of water vapor, $p_w = 2.307 \times 10^{-2}$ atm. The results are shown in Table II.

The partial pressure of water vapor and the temperature strongly modify the evolution surface area–time during dehydration but do not show any influence on the surface area–weight loss relationship in the temperature range 673 K $\leq T \leq$ 773 K and partial pressure of water vapor range 1.683×10^{-2} atm $\leq p_w \leq 3.126 \times 10^{-2}$ atm investigated in this work, as is shown in Figure 2.

The experimental results for the surface area evolution when commercial calcium hydroxide is treated at 683, 698, and 713 K and $p_w = 2.307 \times 10^{-2}$ atm are presented in Figure 3.

An initial zone up to 5% weight loss is observed in Figure 3, with a nonlinear relationship between specific surface area and weight loss (ΔW) changing to a straight line at higher values of ΔW. The presence of the former nonlinear zone has been explained through the coexistence of two different mechanisms corresponding to solid decomposition and recrystallization of the formed crystallites. When the decomposition degree is low, recrystallization is assumed to be the controlling phenomenon in which

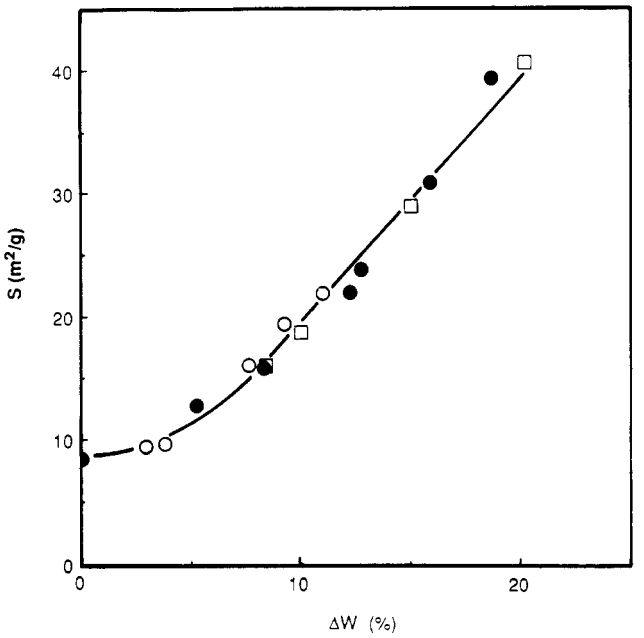

Figure 3. Surface area–weight loss evolution for commercial $Ca(OH)_2$. (○) T = 410 °C; (●) T = 425 °C; (□) T = 440 °C; $p_w = 2.357 \times 10^{-2}$ atm.

Table III. Parameters of the Linear Relationship between S and $(w_0 - w)/w_0$, Equation 5

product	a, $m^2 \cdot g^{-1}$	b, $m^2 \cdot g^{-1}$
commercial $Ca(OH)_2$	0.106	197.45
high surface $Ca(OH)_2$	17.45	98.89

there is not a significant variation in surface area, whereas at higher degrees of decomposition this stage controls the global process, resulting in an evolution of the surface area proportional to the lost water during the dehydration.

A linear model given by eq 5 is able to describe the linear relationship between specific surface area and loss of water:

$$S = a + b\frac{w_0 - w}{w_0} \tag{5}$$

Linear regression fitting of the experimental results for commercial calcium hydroxide, $(w_0 - w)/w_0 > 0.05$ and the high surface area calcium hydroxide according to eq 5, leads to the fitting parameters given in Table III.

From the observation of these results, it is possible to conclude that surface area generation during dehydration at low temperatures $T \leq 773$ K and medium humidity 1.68–3.12% depends mainly on the characteristics of the initial calcium hydroxide and dehydration conversion. An initial activation step seems to be necessary for calcium hydroxide of low specific surface area (commercial) that has not been found in high surface area calcium hydroxide dehydration.

In order to describe the surface area generation during dehydration, conversion–time evolution should be described by the dehydration kinetic model previously developed, eq 6 (Irabien et al., 1990), where the coupling between mass transfer and the kinetic equation needs to be solved for the laboratory or industrial conditions:

$$dx/dt = K_{S0} \exp(-E_a/RT) S_0 (1 - x)[p^*_0 \exp(-\Delta H/RT) - p_w] \tag{6}$$

Therefore, it can be concluded that in the case where sintering during dehydration is negligible, thus, at temperatures below 773 K, the specific surface area of the dehydrated product can be described by eq 5, where fitting parameters depend on the characteristics of the initial calcium hydroxide.

Table IV. Initial Rate of Surface Area Decrease during Sintering

T, K	873	973	1073	1173
$-r_{S0}$, $m^2 \cdot g^{-1} \cdot min^{-1}$	1.915	3.014	3.677	4.276

Table V. Parameters of the Fitting of Experimental Data at 873 and 973 K to Equation 8

	kinetic parameters			
T, °C	c	d	f	std dev, σ
600	0.061	1.741	0.188	2.73
700	0.661	3.060	0.152	2.26

Table VI. Parameters of the Fitting of Experimental Data to the Model of German and Munir, Equation 9, for $\Delta S/S_0 \leq 55\%$

T, °C	γ_S	$10^3 K_i$	r^2
500–600	2.92	1.86	0.92
700	3.64	5.19	0.91

Sintering Modeling. Sintering experiments were performed with completely dehydrated calcium hydroxide (30 min, 723 K) of high surface area ($S \approx 46$ $m^2 \cdot g^{-1}$) in the previously described setup working at temperatures between 773 and 1073 K and at a partial pressure of water vapor $p_w = 2.307 \times 10^{-2}$ atm since sintering was not sensitive to this variable in the researched range: 1.683×10^{-2} atm $\leq p_w \leq 3.126 \times 10^{-2}$ atm.

Experimental surface area–time data are shown in Figures 4 and 5 distinguishing two different zones: the first one at short heating times with a sharp decrease in surface area and the second one at longer times with a slight variation in surface area.

A first approach to calculate the initial rate of surface area loss in the researched range of temperatures was made by evaluating the initial rate values, Table IV, which changed under the studied conditions from 1.9 to 4.2 $m^2 \cdot g^{-1} \cdot min^{-1}$. The influence on the degree of desulfurization of this loss in surface area depends very much on the rate of the sulfation reaction between SO_2 gas and the calcined CaO solid.

For the kinetic analysis of sintering, a general model that accounted for the considerations reported in the literature (Nicholson, 1965; Ranade and Harrison, 1979 Gregg et al., 1955; Sestak, 1984) was analyzed at first

$$dS/dt = -K_S S^m t^{-n} \tag{7}$$

and after integration

$$S^c = S_0^c - dt^f \tag{8}$$

where S and S_0 are the surface areas at $t = t$ and $t = 0$, respectively, and the constants c, d, and f are related to the parameters of eq 7 through the expressions

$$c = 1 - m$$

$$d = K_S(1 - m/1 - n)$$

$$f = 1 - n$$

Nonlinear regression fitting based on the Marquardt optimization subroutine of the experimental data to eq 8 gave the parameters of Table V for the experiments carried out at 873 and 973 K, but poor fittings were obtained with experimental data at 1073 and 1173 K.

In the particular case where $m = 0$, eq 7 takes the form of the model proposed by German and Munir (1976)

$$S/S_0 = 1 - k_i^{1/\gamma_S} t^{1/\gamma_S} \tag{9}$$

A plot of ln $(1 - S/S_0)$ vs ln t is shown in Figure 6. Linear regression fitting of the data for surface reduction less than 55% leads to the parameters of Table VI and for

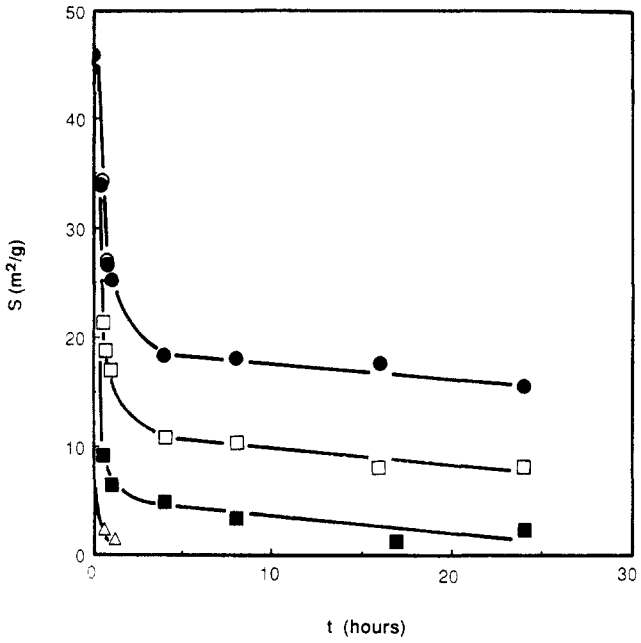

Figure 4. Decrease in surface area as a result of sintering at long times. (○) T = 500 °C; (●) T = 600 °C; (□) T = 700 °C; (■) T = 800 °C; (△) T = 900 °C.

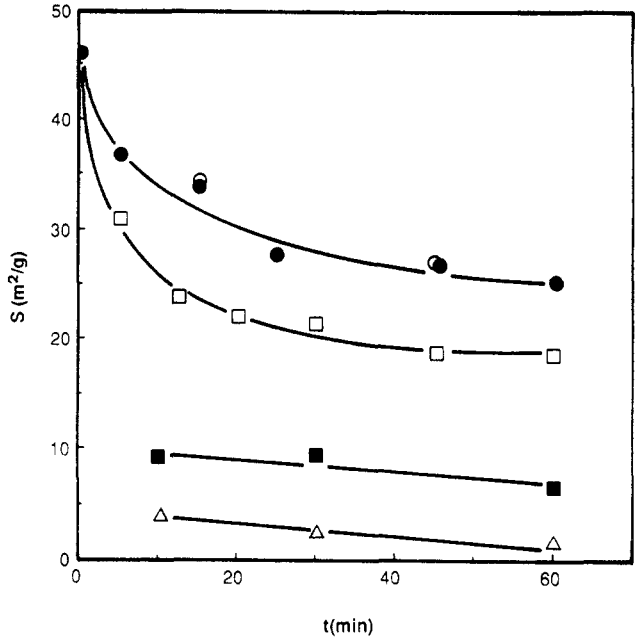

Figure 5. Decrease in surface area as a result of sintering at short times. (○) T = 500 °C; (●) T = 600 °C; (□) T = 700 °C; (■) T = 800 °C; (△) T = 900 °C.

Table VII. Parameters of the Fitting of Experimental Data to the Model of German and Munir, Equation 9, for $\Delta S/S_0 \geq 55\%$

T, °C	γ_S	K_i	r^2
500–600	22.2	4.12×10^{-8}	0.72
700	23.8	7.30×10^{-6}	0.90
800	24.4	2.96×10^{-4}	0.95
900	30.3	6.34×10^{-3}	0.99

Table VIII. Summary of the Kinetic Expressions for Sintering

T, K	kinetic model		kinetic parameters
	$S > 0.45S_0$	$S < 0.45S_0$	
773–873	$S = S_0[1 - K_i^{1/\gamma_S} t^{1/\gamma_S}]$	$S = h + jt$	$K_i = 1.86 \times 10^{-3}$ $\gamma_S = 2.92$ $h = 19.09$ $j = 2.1 \times 10^{-3}$
973	$S = S_0[1 - K_i^{1/\gamma_S} t^{1/\gamma_S}]$	$S = h + jt$	$K_i = 5.19 \times 10^{-3}$ $\gamma_S = 3.64$ $h = 11.04$ $j = -2.2 \times 10^{-3}$
1073		$S = h + jt$	$n = 4.78$ $j = -2.2 \times 10^{-3}$
1173		$S = h + jt$	$h = 4.25$ $j = 49.5 \times 10^{-3}$

surface reduction higher than 55% to parameters of Table VII. In the first case, a mean value of $\gamma_S = 3.28 \pm 0.36$ can be considered for identifying grain boundary diffusion as the mechanism of solid transport, but for $\Delta S/S_0 \geq 55\%$ the obtained values of γ_S are very high (mean value γ_S = 25.2 ± 5) as a result of the interaction between close necks at large times of sintering, which on the other hand is in good agreement with the restrictions of the model of German and Munir.

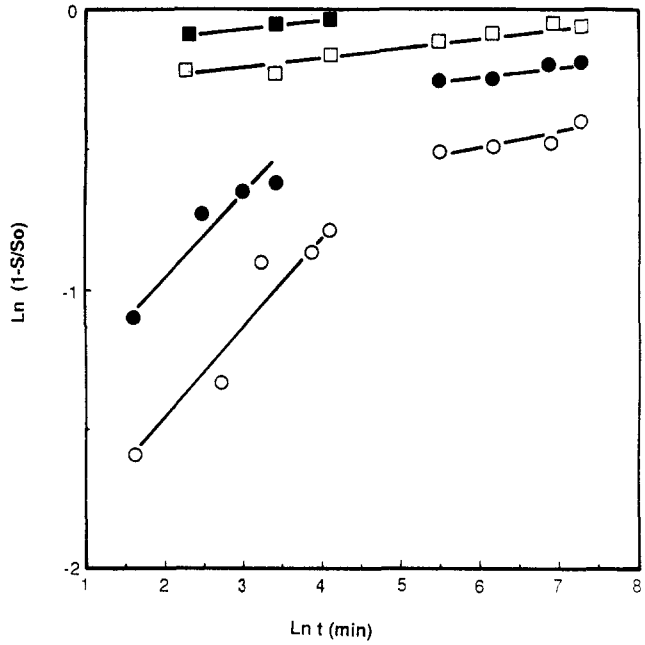

Figure 6. ln $(1 - S/S_0)$ vs ln t. (○) T = 600 °C; (●) T = 700 °C; (□) T = 800 °C; (■) T = 900 °C.

Table IX. Experimental and Simulated Specific Surface Area Data for Sintering

	at 873 K		at 973 K		at 1073 K		at 1173 K	
t, min	exptl	sim	exptl	sim	exptl	sim	exptl	sim
5	36.6	33.5	30.7	26.14				
10	34.0	32.1	27.2	25.1	9.2	4.8	4.0	3.75
15	33.9	30.9	23.7	23.7	8.5	4.75	3.1	3.2
30	27.5	29.5	22.0	22.1	9.3	4.7	2.3	2.8
60	25.2	26.8	16.8	18.4	6.5	4.6	1.45	1.28
240	18.3	21.8	10.6	13.2	4.9	4.2		
480	18.1	18.9	10.2	10.5	3.4	3.7		
960	17.6	15.8	8.2	7.7	2.5	2.8		
1020	16.5	15.0	8.0	7.2	1.4	2.5		
1440	15.7	13.9	8.2	6.1	2.3	1.6		

An empirical linear model correlating the specific surface area data at long heating times was taken. Table VIII summarizes the kinetic expressions and parameters describing the evolution of surface area loss when an initial calcium oxide with $S \approx 46$ $m^2 \cdot g^{-1}$ is thermally treated at temperatures in the range 773–1173 K, and in Table IX a good agreement of the experimental and simulated data employing the kinetic expressions of Table VIII is observed, thus checking the validity of the reported kinetic expressions in order to describe the loss in surface area of calcium oxide due to sintering phenomena.

Conclusions

Structural changes in the solid sorbent used in dry desulfurization processes are related to the yield of the gas–solid reactions. If calcium hydroxide is used as the solid sorbent, three different phenomena are associated with the change in surface area: first, a surface area generation depending on the dehydration reaction to give a highly porous calcium oxide; second, a surface area reduction due to sintering; and third, the surface change due to the sulfation reaction.

The coupling between surface area generation and sintering can only be solved at temperatures below 773 K. The dehydration results of this work obtained under constant partial pressure of water for commercial calcium hydroxide ($S_0 \approx 8.3$ $m^2 \cdot g^{-1}$) and high surface calcium hydroxide ($S_0 \approx 18.7$ $m^2 \cdot g^{-1}$) indicate that surface area generation can be fitted by a linear equation (eq 5) but parameters depend strongly on the initial calcium hydroxide.

Borgwardt (1989) evaluated the surface area of nascent calcium oxide obtained from different precursors after 5 min of dehydration at 700 °C in pure nitrogen, obtaining an experimental value of 76.7 $m^2 \cdot g^{-1}$. The difference between 76.7 $m^2 \cdot g^{-1}$ (Borgwardt, 1989) and 46 $m^2 \cdot g^{-1}$ obtained in this work may be attributed to the influence of the partial pressure of water vapor in the characteristics of calcium oxide and/or to the influence of the starting material.

An estimation of the quantitative meaning of sintering has been performed by evaluating the initial rates of surface decrease in experiments between 873 and 1073 K, obtaining the values 1.9 $m^2 \cdot g^{-1} \cdot min^{-1} \leq (-dS/dt)_0 \leq 4.2$ $m^2 \cdot g^{-1} \cdot min^{-1}$, which demonstrate the coupling between surface generation by dehydration and surface decrease by sintering at temperatures above 773 K.

The model reported by German and Munir (1976) and applied previously by Borgwardt (1989) satisfactorily correlated experimental data of completely dehydrated commercial calcium hydroxide ($S \approx 46$ $m^2 \cdot g^{-1}$) at defined values of the partial pressure of water, 1.683×10^{-2} atm $\leq p_w \leq 3.126 \times 10^{-2}$ atm, when $\Delta S/S_0 \leq 55\%$, obtaining a mean value of the parameter $\gamma_S = 3.28 \pm 0.36$, thus identifying grain boundary diffusion as the mechanism of solid transport.

An empirical model where the surface area is directly proportional to the heating time correlated the experimental results of surface reduction higher than 55%. Simulated curves utilizing the kinetic expressions and reported parameters show good agreement with the experimental data.

The results of this work allow the practical application of surface generation and surface reduction models to desulfurization conditions, where partial pressure of water is not negligible.

Further research on the surface generation and surface decreasing processes at higher and lower partial pressures of water is now under development.

Acknowledgment

This work has been financially supported by the spanish CICYT under Project PA86-0147.

Nomenclature

a, b: empirical parameters defined by eq 5
A: refers to the reagent, calcium hydroxide
B: refers to the product, calcium oxide
c, d, f: parameters defined by eq 8
E_S: energy of activation of sintering, $cal \cdot mol^{-1}$
K_i: sintering rate constant in an inert atmosphere, eq 3, t^{-1}
K_S: rate constant, eq 8, min^{n-1}
K_T: temperature-dependent constant, eq 1
m, n: empirical parameters, eq 7 and eq 2
p_w: water vapor pressure at equilibrium, atm
$-r_S$: surface area referring to the dehydration rate, $mol \cdot m^{-1} \cdot min^{-1}$
S: specific surface area, $m^2 \cdot g^{-1}$
t: time
T: temperature
W: weight fraction
x: dehydration conversion

Greek Letters

γ_S: mechanism-dependent exponent defined by eq 3

Registry No. $Ca(OH)_2$, 1305-62-0; CaO, 1305-78-8.

Literature Cited

Borgwardt, R. H. Sintering of nascent calcium oxide. *Chem. Eng. Sci.* **1989**, *44*, 53–60.

Bortz, S. J.; Roman, V. P.; Yang, R. J.; Flament, P.; Offen, G. R. Precalcination and its Effect on Sorbent Utilization during Upper Furnace Injection. *Abstracts of Papers*, Symposium on Dry SO_2/NO_x Control Technologies, Raleigh, NC, 1986.

Cole, J. A.; Kramlich, J. C.; Seeker, W. R.; Silcox, G. D.; Newton, G. H.; Harrison, D. J.; Pershing, D. W. Fundamental Studies of Sorbent Reactivity in Isothermal Reactors. *Abstract of Papers*, Symposium on Dry SO_2/NO_x Control Technologies, Raleigh NC, 1986.

Feugier, A. Aspects théoriques de la désulfuration en lit fluidisé. *Rev. Inst. Fr. Pet.* **1986**, *3*, 433–440.

German, R. M.; Munir, Z. A. Surface area reduction during isothermal sintering. *J. Am. Ceram. Soc.* **1976**, *59*, 379–383.

Gregg, S. J.; Packer, R. K.; Wheatley, K. H. The Production of Active Solids by Thermal Decomposition. Part V*. The Sintering of Active Magnesium Oxide. *J. Chem. Soc.* **1955**, 46–50.

Irabien, A.; Viguri, J. R.; Ortiz, I. Thermal dehydration of calcium hydroxide. 1. Kinetic Model and Parameters. *Ind. Eng. Chem. Res.* **1990**, preceding paper in this issue.

Mai, M. C.; Edgar, T. F. Surface Area Evolution of Calcium Hydroxide During Calcination and Sintering. *AIChE J.* **1989**, *35*, 30–36.

Nicholson, D. Variation of Surface Area During the Thermal Decomposition of Solids. *Trans Faraday Soc.* **1965**, *61*, 990–998.

Ranade, P. V.; Harrison, D. P. The grain model applied to porous solids with varying structural properties. *Chem. Eng. Sci.* **1979**, *34*, 427–431.

Sestak, J. Sintering and related phenomena. In *Thermophysical properties of solids*; Academia: Prague, 1984.

Silcox, G. D.; Payne, R.; Pershing, D. W.; Seeker, W. R. A comparison of Combustion Facilities and Calcium Based Sorbents in Terms of Their Sulfur Capture Performance. *Abstracts of Papers*, Symposium on Dry SO_2/NO_x Control Technologies, Raleigh, NC, 1986.

Viguri, J. R. Hidroxido de calcio como reactivo en desulfuración de gases: Deshidratación y sinterización. Ph.D. Dissertation, The University of País Vasco, Bilbao, Spain, 1989.

Received for review August 25, 1989
Revised manuscript received March 14, 1990
Accepted April 2, 1990